Transition from chaotic to regular behavior of electrons in a stadium-shaped quantum dot in a perpendicular magnetic field

Zhen-Li Ji and Karl-Fredrik Berggren
Department of Physics and Measurement Technology, Linköping University, S-581 83 Linköping, Sweden
(Received 25 January 1995)

The energy spectrum, wave functions, and field-induced currents in a two-dimensional isolated stadium-shaped dot are calculated in the presence of a perpendicular magnetic field. By means of the magnetic field one can explore the dynamics of this type of system, from quantum chaotic to regular behavior. The distribution of energy-level spacings is found to transform gradually from a Wigner (Gaussian orthogonal ensemble) distribution at zero field to a Poisson distribution as the magnetic field increases. The spatial distributions of the currents and charge densities are used in elucidating and visualizing the gradual formation of bulk Landau states and edge states at high magnetic fields.

I. INTRODUCTION

In ultrasmall semiconductor structures and devices, electrons may be confined to two-dimensional areas of the size of a micron or less.[1,2] When the feature size of a device is made comparable to the electron de Broglie wavelength, the properties of such a device are governed by quantum mechanics. A general feature of electron transport in submicron electronic devices is the appearance of large irregular fluctuations in the conductance when measured at low temperatures. Recently there has been interest in the statistical properties of such fluctuations in ballistic transport within the semiclassical framework of quantum chaotic scattering.[3–8] Theoretical studies have suggested that the chaotic behavior of the conductance is induced by the geometry of the confining potential in cross-shaped junctions and in open stadium billiards, i.e., billiards with open leads attached. Also, measurements of chaotic scattering have been reported for ballistic $GaAs/Al_xGa_{1-x}As$ microstructures.[9] The resistance across a microstructure in the shape of a stadium was measured as a function of applied perpendicular magnetic field. In general the measurements show large nonuniversal conductance fluctuations which may be due to both quantum interference because of, e.g., coherent backscattering and the particular geometry of the device. However, in the tunneling regime, i.e., a stadium that is classically isolated, the magnetoresistance shows periodic oscillations at high magnetic fields.[10,11]

It is known that the motion of a classical particle in a closed stadium is chaotic.[12] Numerous theoretical works have been applied to the understanding of the quantum analog of such systems.[13] In particular, detailed investigations of the quantum behavior in a stadium have shown that the eigenvalue spectrum satisfies the Gaussian orthogonal ensemble (GOE),[14] and most stationary states are concentrated around narrow channels, called scars, which resemble the classical periodic orbits.[15] In spite of all previous theoretical work, the effects of a magnetic field on a closed quantum stadium have not been studied so far in a complete quantum-mechanical way. In view of experiments on nanoscale arenas, studies of this kind are timely.

In this paper we study one-electron states of a stadium billiard in a magnetic field. The energy spectrum, two-dimensional spatial distribution of the current, and charge density are calculated using a numerical approach which is similar to that of Weisz and Berggren.[16] The charge density and current induced by the applied magnetic field are interesting because they contain information about the properties of stadium billiards. The current patterns indicate the transition from chaotic to regular behaviors as the magnetic field is increased. The reason for this is the formation of edge states and bulk Landau states at high magnetic fields. The correspondence between the quantum current flows and classical orbits will be discussed. These results are useful in understanding the recent magnetotransport experiments for stadium-shaped microstructures.[9–11]

The rest of the paper is organized as follows. In Sec. II, we briefly present the theory used in computing the energy spectrum, two-dimensional current, and charge-density profiles. In Sec. III, we examine the energy spectra and the states of a stadium in a magnetic field. Attention is focused on the transition from chaotic to regular at high magnetic fields. Finally, in Sec. IV, we present our conclusions.

II. THEORY

The stadium system considered in our study consists of two semicircles of radius R connected by two parallel, equal, rectilinear intervals of length $2L$ as shown in Fig. 1. Neglecting the effect of spin, the single-particle Hamiltonian for an electron with effective mass $m^*=0.067m_0$, appropriate for GaAs, and charge $-e$, can be written as

$$H=\frac{1}{2m^*}(-i\hbar\nabla+e\,\mathbf{A})^2+V\ , \tag{1}$$

where V is the confinement potential and $\mathbf{A}$ is the vector potential of the external magnetic field $\mathbf{B}$. Here we assume that the electrons are confined by infinite walls. Inside the dot the potential V equals zero. We examine the case of a perpendicular magnetic field $\mathbf{B}=\nabla\times\mathbf{A}=B\hat{\mathbf{z}}$,

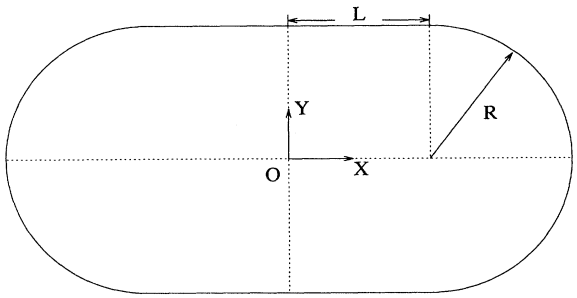

FIG. 1. Schematic diagram for a stadium billiard where the radius of the semicircle is $R=50$ nm, and the length of the rectangle is $2L=2R$.

and use the symmetric gauge for the vector potential:

$$\mathbf{A}=\left[-\frac{By}{2},\frac{Bx}{2},0\right] . \tag{2}$$

The Schrödinger equation can then be written in the form

$$\frac{1}{2m^*}\left[\left[-i\hbar\frac{\partial}{\partial x}-\frac{eBy}{2}\right]^2+\left[-i\hbar\frac{\partial}{\partial y}+\frac{eBx}{2}\right]^2\right]\Psi =(E-V)\Psi . \tag{3}$$

One can simply replace the derivatives in Eq. (3) by symmetric difference approximations

$$\frac{\partial}{\partial x}\Psi\approx\frac{\Psi_{i+1,j}-\Psi_{i-1,j}}{2\Delta x} , \tag{4a}$$

$$\frac{\partial^2}{\partial x^2}\Psi\approx\frac{\Psi_{i+1,j}-2\Psi_{i,j}+\Psi_{i-1,j}}{(2\Delta x)^2} , \tag{4b}$$

$$\frac{\partial}{\partial y}\Psi\approx\frac{\Psi_{i,j+1}-\Psi_{i,j-1}}{2\Delta y} , \tag{4c}$$

$$\frac{\partial^2}{\partial y^2}\Psi\approx\frac{\Psi_{i,j+1}-2\Psi_{i,j}+\Psi_{i,j-1}}{(2\Delta y)^2} . \tag{4d}$$

The grid problem with N nodes in the stadium turns into an $N\times N$ eigenvalue problem. This results from regarding the $\Psi_{i,j}$ as stored into a vector $C_n(n=1,2,\ldots,N)$ and then solving the eigenvalue problem $HC=EC$. It is important to have a fine mesh in the stadium to ensure numerical accuracy. Results for the eigenvalues may be checked for convergence as the node number N is made larger. The lowest eigenvalues converge faster and are the therefore more reliable. For a size of the stadium with $R=50$ nm and magnetic field $B\leq 7$ T considered here, we have used 8991 nodes for computing the 25 lowest eigenvalues. Meshes of up to 32 613 nodes were used to achieve convergence for the 400 lowest eigenvalues.

For each eigenstate, the two-dimensional electron probability density $\rho(x,y)$ and current density $\mathbf{J}(x,y)$ are calculated directly from the computed wave functions $\Psi(x,y)$ through the relations

$$\rho(x,y)=|\Psi(x,y)|^2 , \tag{5}$$

$$\mathbf{J}(x,y)=-\frac{\hbar}{m^*}\mathrm{Im}[\Psi(x,y)\nabla\Psi^*(x,y)]+\frac{e}{m^*}\mathbf{A}|\Psi(x,y)|^2 . \tag{6}$$

III. NUMERICAL RESULTS

A. The energy spectrum

We have calculated the magnetic-field dependence of the electron energies in a quantum stadium using the symmetric gauge calculated by discretizing the Schrödinger equation.[16] Figure 2 shows the eigenvalue spectrum as a function of applied magnetic field for the first 25 eigenstates. At high magnetic fields the condensation of the states into degenerate bulk Landau levels is evident. In this limit we also recognize levels that are associated with edge states. At low magnetic fields the spectrum is quite complicated. Both crossing and anticrossing of the energy levels occur in the figure. Anticrossing occurs for states belonging to the same symmetry class, while states from different classes may cross. In the integrable systems, such as a circular dot, only crossing occurs.[17,18] Anticrossing or level repulsion results from the nonintegrability of our problem and is a signature of quantum chaos. The repulsion becomes weaker as the magnetic field is increased in Fig. 2. In Fig. 3 we show the Fermi energy as a function of the magnetic field for the stadium with different numbers of noninteracting electrons at zero temperature. The Fermi energy is not a smooth function of the magnetic field. The convergence to the lowest Landau-level energy is much faster for stadia with a smaller number of electrons.

B. Charge density and current flow

Robnik and Berry studied the classical problem of a charged particle moving in a closed planar billiard with sufficiently smooth boundaries in a magnetic field.[19] They found that the type of dynamics depends on the value of applied magnetic field in relation to the radii of

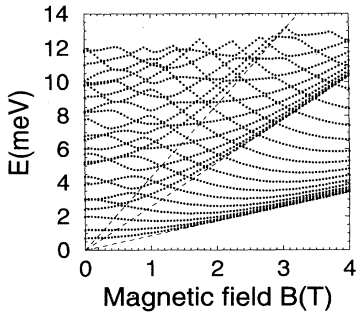

FIG. 2. The energy levels as a function of the magnetic field for the stadium-shaped quantum structure. The Landau-level energies of an ideal two-dimensional system (dashed lines) are given as a reference.

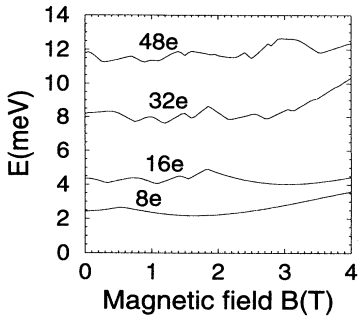

FIG. 3. Fermi energy as a function of the magnetic field for different numbers of electrons.

curvature of the boundary. For a quantum stadium billiard, an interesting question is how the applied magnetic field affects the charge density and current flow pattern.

In Figs. 4(a)–4(f) we show how the charge density and current flow pattern of the 24th-lowest state in energy evolve with increasing magnetic field. At $B=0.01$ T the charge density in Fig. 4(a) is, of course, similar to that calculated for a stadium at zero magnetic field.[20] For higher states the density distribution becomes more complex because more nodes appear. Patterns of this kind are also observed experimentally for quantum corrals by means of the scanning tunneling microscope (STM).[21]

As shown in Fig. 4(b) the currents induced by the field show a volatile vortical pattern as one would expect in a chaotic regime. In fact, the results are reminiscent of the current distributions associated with transport in a cross-bar device.[22] Figure 4(c) and 4(d) show a hybrid state where vortical and regular regions coexist at an intermediate field of 1.3 T. At a high magnetic field, the state has already condensed, i.e., it has transformed into a bulk Landau state in this case. The charge density and current pattern in Figs. 4(e) and 4(f) clearly show that the charge density peaks near the center of the stadium at $B=2.9$ T. The behavior can be understood as a localization of the wave function at the center of the stadium due to magnetic confinement applied on the electrons. Figures 4(a)–4(f) show that an applied magnetic field may be used to explore the transition from quantum

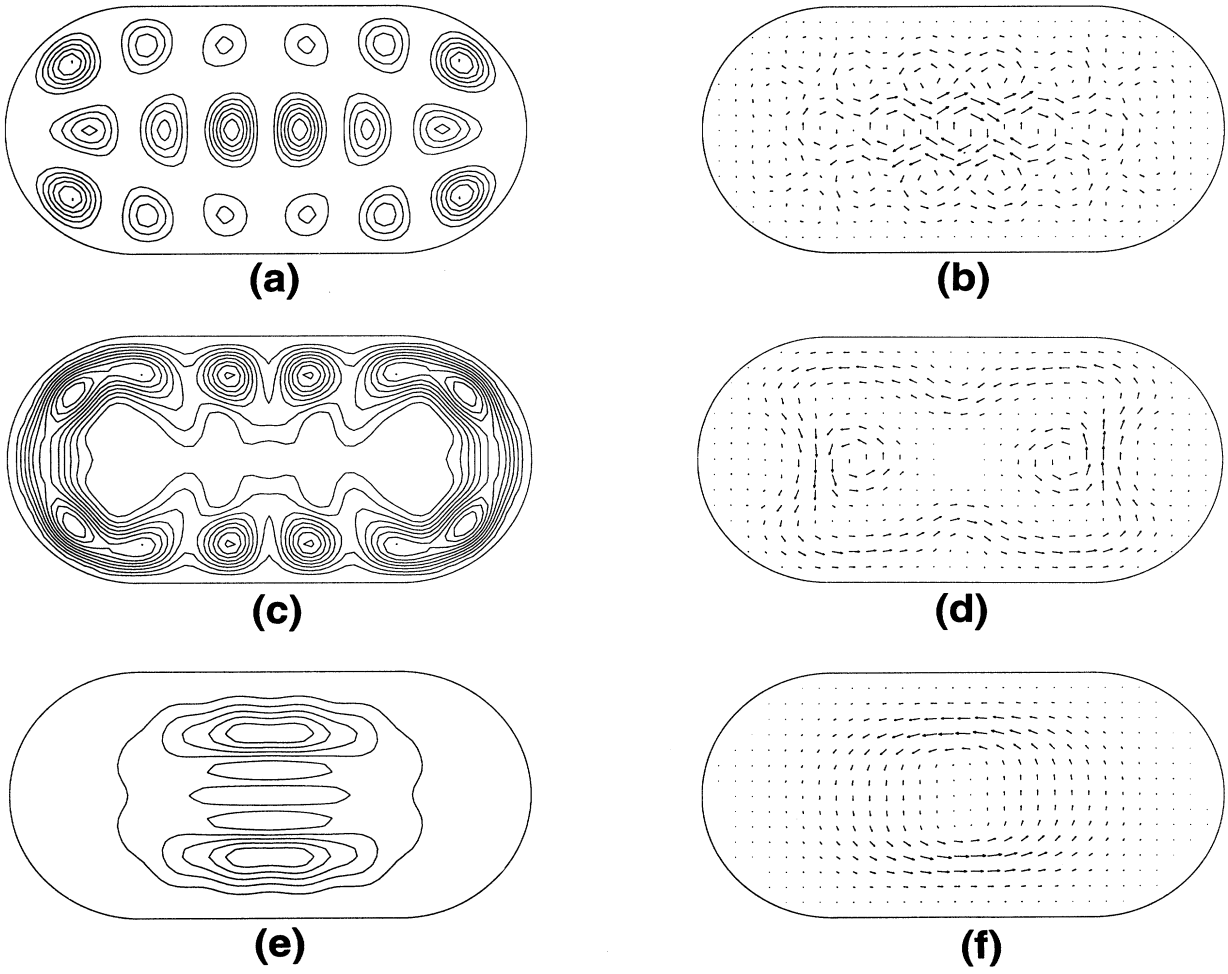

FIG. 4. The charge density and current flow pattern of 24th-lowest state in energy for different magnetic field. (a) and (b) $B=0.01$ T. (c) and (d) $B=1.3$ T. (e) and (f) $B=2.9$ T.

chaotic→mixed→regular dynamics which was observed in the recent experiment mentioned.[10,11] We also found this kind of transition from chaotic to regular for other states in the stadium. As expected, the transition from chaotic to regular occurs at lower fields for lower-energy states. The reason is that, for lower energies, the effect of the magnetic confinement more easily overcomes the geometric confinement.

C. Connection to classical orbits

The current flow shown in Fig. 4(f) corresponds to the classical picture of counter-clockwise orbit caused by the Lorenz force on the electron. However, the state shown in Fig. 5(a) is somewhat surprising. Rather than a counterclockwise current flow, there is a clockwise circulation in the stadium. To understand the physics underlying this behavior, Lent[18] studied the problem of a charged particle moving in a circular quantum dot in a perpendicular magnetic field, and examined the correspondence between quantum current flows and classical orbits using approximate expressions for the guide-center radius and cyclotron radius. For a stadium billiard, we would expect a similar case. The classical orbits for the stadium corresponding to quantum states in Figs. 5(a) and 5(b) are illustrated in Figs. 5(c) and 5(d), respectively. As the magnetic field increases, both the radius of the cyclotron orbit and the distance from guiding center to origin become smaller. Because of the effect of the stadium walls, the orbits of guiding centers (dotted) in Figs. 5(c) and 5(d) are not as circular as that in the unconfined Landau system. One notes that the current in Fig. 5(a) is characteristic of a pure edge state corresponding to a skipping orbit. This is consistent with periodic oscillations in the high-field magnetoresistance observed in the tunneling regime.[11] Tunneling takes place to the outermost edge states only because the overlap with the inner states is negligible. When the magnetic field **B** is increased, additional edge states become populated consecutively, causing the Aharonov-Bohm-type oscillations. At the same time lower edge states move into the central region to become bulk Landau states.

D. Distribution of energy-level spacings

Let us now turn to the distribution of the eigenvalue spectrum in the stadium. A statistical description of the spectrum in terms of the probability distribution of neighboring level separations has received particular attention for quantum chaos.[14,23,24] In applying a statistical description to a chaotic situation, it is important that any discrete symmetries of the problem be taken into account. The geometry of the stadium billiard shown in Fig. 1 has vertical and horizontal symmetry lines. Solutions of the Schrödinger equation in this stadium can be broken into classes according to whether they are even or odd about the symmetry lines. There are four symmetry classes at $B=0$ T, as shown in Fig. 6. The problem can be reduced to solve the Schrödinger equation in a quarter of the original billiard area with conditions on boundaries Γ_1, Γ_2, and Γ_3 (see the caption of Fig. 6).

The distribution $P(s)$ of eigenvalue spacings is one statistical measure of the spectrum. It is defined so that s is the level spacing divided by its mean $\langle s \rangle$, and $P(s)ds$ is

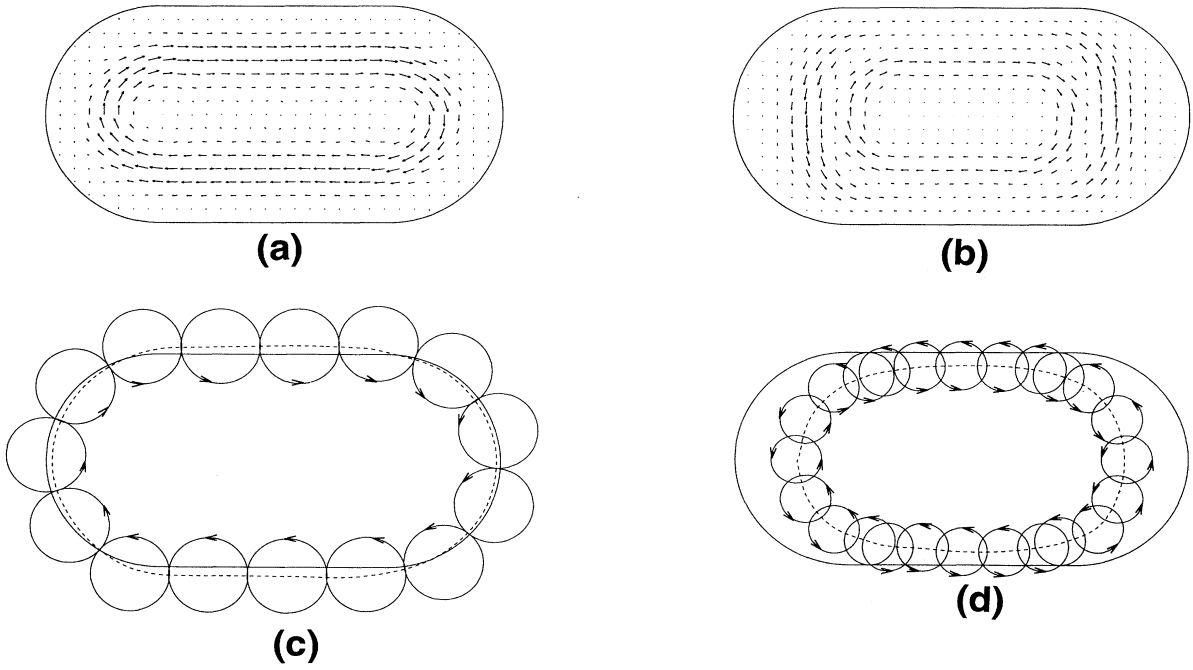

FIG. 5. (a) The current distribution of the eighth-lowest state in energy at $B=2$ T. (b) The current distribution of the eighth-lowest state in energy at $B=4$ T. The classical orbits for the stadium corresponding to quantum-mechanical eigenstates of (a) and (b) are illustrated in (c) and (d), respectively.

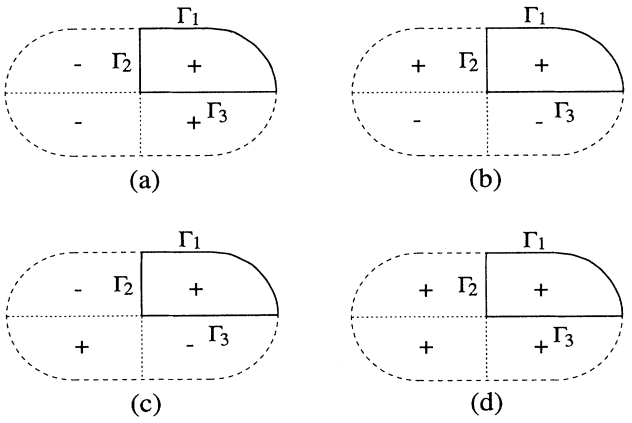

FIG. 6. The symmetry classes of solutions of the Schrödinger equation in a stadium correspond to a quarter of the stadium with different boundary conditions. (a) $\Psi(x,y)=0$ on Γ_1 and Γ_2, and $\partial\Psi(x,y)/\partial y=0$ on Γ_3. (b) $\Psi(x,y)=0$ on Γ_1 and Γ_3, and $\partial\Psi(x,y)/\partial x=0$ on Γ_2. (c) $\Psi(x,y)=0$ on Γ_1, Γ_2, and Γ_2. (d) $\Psi(x,y)=0$ on Γ_1, $\partial\Psi(x,y)/\partial x=0$ on Γ_2, and $\partial\Psi(x,y)/\partial y=0$ on Γ_3.

the probability of finding a separation of neighboring levels between s and $s+ds$. Histograms are shown in Fig. 7 for different symmetry classes. Figure 7(a), 7(b), and 7(c) correspond to symmetry classes shown in Figs. 6(a), 6(b), and 6(c), respectively. As can be seen, distributions of eigenvalue spacings for different symmetry classes very closely follow the GOE distribution $P(s)=(\pi s/2)\exp(-\pi s^2/4)$.[13,17] Small spacings are less probable; also large spacings are improbable. The spectrums exhibit apparent mutual repulsion of eigenvalues. For each symmetry class the 400 lowest levels have been included in the analysis. We have also used 400–1500 eigenvalues for the histogram in the case of Fig. 7(c), and checked that essentially the same results were obtained upon increasing the number of eigenvalues. Figure 7(d) shows the average of histograms shown in Figs. 7(a), 7(b), and 7(c). The histogram appears to agree well with GOE statistics.

For sufficiently strong magnetic field, the level spacing distribution is expected to be the Gaussian unitary ensemble (GUE) statistics $P(s)=(32/\pi^2)s^2\exp[-(4/\pi)s^2]$ due to the breaking of time-reversal symmetry.[17] The geometry of Fig. 1 admits reflection symmetries at origin O, which give rise to odd and even parities of the solutions, i.e., the symmetry is lowered relative the field-free case. We have examined the distributions of nearest-neighbor spacings for both parities, and found that they

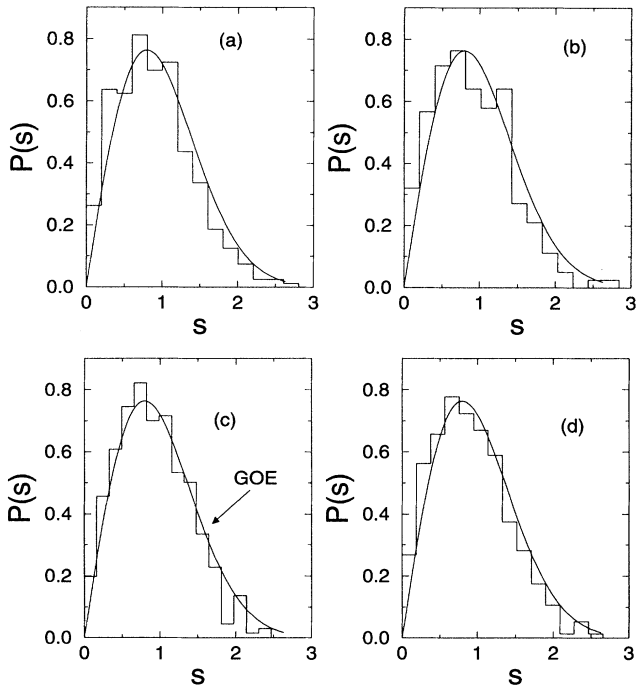

FIG. 7. Distributions of energy-level spacings for a stadium. 400 levels have been included in the analysis corresponding to the first to the 400th levels for different symmetry classes. Histograms shown in (a), (b), and (c) correspond to the symmetry classes shown in Figs. 6(a), 6(b), and 6(c), respectively. The histograms for the average values of (a), (b), and (c) are shown in (d). Smooth curves: Wigner distribution.

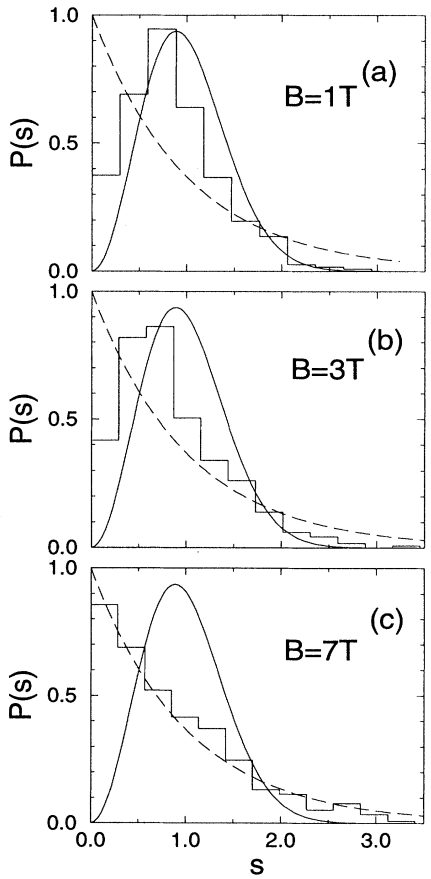

FIG. 8. Histogram: the distributions of (odd parity) energy-level spacings. Solid and dashed lines: GUE and Poisson distributions, respectively. The magnetic field B varies as follows: (a) $B=1$ T, (b) $B=3$ T, and (c) $B=7$ T. 400 odd-parity eigenvalues have been included in the analysis.

have similar statistical properties.

At very low fields the states are very close to the unperturbed case. The distribution we find is therefore essentially the same as if we would have combined (a) and (b), or (c) and (d), in Fig. 6 in the analysis of level spacings at $B=0$. The distribution essentially reflects both Poisson- and Wigner-like statistics. With increasing B the mixing of (a) with (b) and (c) with (d) increases and causes further level repulsion. Hence we should anticipate GUE-like statistics at some field.

In Fig. 8, we plot histograms of the nearest-neighbor interlevel spacings for three different magnetic fields of $B=1$, 3, and 7 T together with lines corresponding GUE and Poisson distributions. For the lower magnetic field [Fig. 8(a)] the distribution is close to the one for the GUE statistics. However, the perfect GUE form never develops in our case, because regular Landau bulk states occur at low energies. For the higher magnetic field [Fig. 8(c)], the distribution is close to a Poisson distribution $P(s)=\exp(-s)$ expected for a regular system. Clearly, a transition from the GUE-like to the Poisson distribution is taking place.

IV. CONCLUSIONS

Numerical solutions of the Schrödinger equation for an electron in a quantum stadium have been performed. We have examined the spatial distributions of current and charge density in the presence of a magnetic field. We show how the charge density and current pattern in the stadium evolve, and how electron motion changes from chaotic to regular with increasing magnetic field. At high magnetic fields, both counter-clockwise and clockwise current flows are found. The correspondence between quantum current flows and classical orbits was discussed. The energy spectrum is analyzed in terms of the probability of neighboring energy-eigenvalue separations, which is shown to be similar to a GOE distribution at $B=0$, a GUE-like distribution at intermediate magnetic fields, and a Poisson distribution at high magnetic fields.

Our results are consistent with recent measurements of the magnetoresistance in the tunneling regime. The field at which the transition is completed is, however, different compared with experiments because of differences in the dimensions of the dot and Fermi energy. Another reason is the shape of the confining walls. Here we have used infinite walls, but in a real device one should expect a smooth confinement. A more realistic modeling consists of a parabolic potential outside a stadium-shaped flat region. This point needs further investigation, but preliminary calculations show that softness could play a role. There are also other features of the potential that we have chosen to ignore here. In a real device one should expect small deviations from the perfect, lithographically defined shape. Since the appearance of quantum chaos is related to the removal of symmetry, small irregularities of this kind can have a profound impact on the level statistics.[25] Random potential fluctuations due to, e.g., donor ions will act in the same way. Features like these should not change, however, the overall picture of a crossover from quantum chaotic to regular behavior with increasing magnetic field.

ACKNOWLEDGMENTS

We gratefully acknowledge the support of the Swedish Engineering and Natural Science Research Councils.

[1] *Nanostructure Physics and Fabrication,* edited by M. A. Reed and W. P. Kirk (Academic, New York, 1989).
[2] C. W. J. Beenakker and H. van Houten, in *Solid State Physics,* edited by H. Ehrenreich and D. Turnbull (Academic, San Diego, 1991), Vol. 44, p. 1, and references cited therein.
[3] R. A. Jalabert, H. U. Baranger, and A. D. Stone, Phys. Rev. Lett. **65**, 2442 (1990).
[4] R. V. Jensen, Chaos **1**, 101 (1991).
[5] R. B. S. Oakeshott and A. MacKinnon, Superlatt. Microstruct. **11**, 145 (1992).
[6] H. U. Baranger, D. P. DiVincenzo, R. A. Jalabert, and A. D. Stone, Phys. Rev. B **44**, 10 637 (1991).
[7] W. A. Lin and J. B. Delos, Chaos **3**, 655 (1993).
[8] K. Nakamura and H. Ishio, J. Phys. Soc. Jpn. **61**, 3939 (1992).
[9] C. M. Marcus, A. J. Rimberg, R. M. Westervelt, P. F. Hopkins, and A. C. Gossard, Phys. Rev. Lett. **69**, 506 (1992).
[10] C. M. Marcus, R. M. Westervelt, P. F. Hopkins, and A. C. Gossard, Chaos **3**, 643 (1993).
[11] C. M. Marcus, R. M. Westervelt, P. F. Hopkins, and A. C. Gossard, Surf. Sci. **305**, 480 (1994).
[12] M. Gutzwiller, *Chaos in Classical and Quantum Mechanics* (Springer-Verlag, New York, 1991).
[13] *Chaos and Quantum Physics,* edited by M.-J. Giannoni, A. Voros, and J. Zinn-Justin (Elsevier, London, 1990), and references cited therein.
[14] S. W. McDonald and A. N. Kaufman, Phys. Rev. Lett. **42**, 1189 (1979).
[15] E. J. Heller, Phys. Rev. Lett. **53**, 1515 (1986); E. J. Heller, P. W. O'Connor, and J. Gehlen, Phys. Scr. **40**, 354 (1989).
[16] J. F. Weisz and K.-F. Berggren, Phys. Rev. B **41**, 1687 (1990).
[17] E. Ott, *Chaos in Dynamical Systems* (Cambridge University Press, Cambridge, 1993).
[18] C. S. Lent, Phys. Rev. B **43**, 4179 (1991).
[19] M. Robnik and M. V. Berry, J. Phys. A **18**, 1361 (1985).
[20] M. Shapiro, Chem. Phys. Lett. **106**, 325 (1984).
[21] E. J. Heller, M. F. Crommle, C. P. Lutz, and D. M. Eigler, Nature **369**, 464 (1994).
[22] K.-F. Berggren, C. Besev, and Zhen-Li Ji, Phys. Scr. **T42**, 141 (1992).
[23] S. W. McDonald and A. N. Kaufman, Phys. Rev. A **37**, 3067 (1988).
[24] O. Bohigas, M. J. Giannoni, and C. Schmit, Phys. Rev. Lett. **52**, 1 (1984).
[25] A. D. Stone and H. Bruus, Physica B **189**, 43 (1993).